4

Nuclear Factor-κB pathway-activating gene aberrancies in primary cutaneous large B-cell lymphoma, leg type

Abridged version published:

Journal of Investigative Dermatology 2014; 134(1): 290-292

Lianne Koens[1]

Willem H. Zoutman[2]

Passorn Ngarmlertsirichai[3]

Grzegorz K. Przybylski[3,4]

Piotr Grabarczyk[3]

Maarten H. Vermeer[2]

Rein Willemze[2]

Patty M. Jansen[1]

Christian A. Schmidt[3]

Cornelis P. Tensen[2]

Departments of [1]Pathology; and [2]Dermatology, Leiden University Medical Center, Leiden, The Netherlands;

[3]Clinic for Internal Medicine C , University Greifswald, Greifswald, Germany and [4]Instute of Human Genetics, Polish Academy of Sciences, Poznan, Poland

4

Abstract

Primary cutaneous large B-cell lymphoma, leg type (PCLBCL-LT) is an aggressive cutaneous lymphoma with a 5-year overall survival of approximately 40%. At gene expression level, PCLBCL-LT resembles the activated B-cell (ABC)type of nodal diffuse large B-cell lymphoma (DLBCL). In ABC-DLBCL, a role for constitutive Nuclear Factor (NF)-κB pathway activation in tumor cell survival is generally recognized. We screened 10 cases of PCLBCL-LT for genetic alterations potentially leading to aberrant NF-κB activation. Tumor suppressor gene TNFAIP3 was heterozygously deleted in four cases. No additional promoter hypermethylation was detected. A CD79BY196 mutation was found in 2 cases. The coiled-coil domain of CARD11 contained a D415E and a R423W mutation in one sample. At genomic level, the oncogenic MYD88 L265P mutation was found in 4 cases, of which 3 showed the same mutation at transcriptional level. Combined, seven out of 10 cases of PCLBCL-LT showed genetic alterations in genes that regulate NF-κB activation. The percentages of mutations were highly concordant with those encountered in nodal ABC-DLBCL. Together, these findings strongly suggest a role for constitutive activation of the NF-κB pathway in PCLBCL-LT and provide the rationale to explore using new treatment modalities targeted at components of the NF-κB pathway.

Introduction

Primary cutaneous large B-cell lymphoma, leg type (PCLBCL-LT) is an aggressive cutaneous lymphoma with a 5 year overall survival of approximately 40%.[1] Due to its aggressive nature, the treatment of first choice is anthracyclin-based chemotherapy combined with rituximab.[2] However, patients often show a progressive disease course despite treatment with polychemotherapy. Furthermore, due to age and (age-related) comorbidity, not all patients are eligible for this treatment. Therefore, new and additional therapies for PCLBCL-LT are necessary, with a focus on more specific, targeted therapies with fewer side effects than conventional chemotherapy.

At mRNA expression level, PCLBCL-LT resembles activated B-cell (ABC) type of nodal diffuse large B-cell lymphoma (DLBCL), including strong expression of known targets of the Nuclear Factor (NF)-κB pathway, such as interferon regulatory factor 4(*IRF4)*.[3-5] In nodal ABC-type/non-germinal center-type DLBCL, increased NF-κB activity likely plays a role in its pathogenesis, by acting as a transcription factor involved in several cellular survival mechanisms. In line with this role, in nodal ABC-type DLBCL cell lines, constitutive activation of NF-κB is required for tumor cell survival.[3,6] Studies on the molecular background of NF-κB pathway activation have demonstrated that mutations in multiple genes can cause deregulation of NF-κB signaling in nodal ABC-type DLBCL.[7] The genes most frequently affected by genetic aberrations are *TNFAIP3 (A20)*, *CD79B*, *CARD11 (CARMA1)*, and *MYD88*, which all can contribute to constitutive activation of the NF-κB pathway. In two-third of cases nodal ABC-type DLBCL, one or more of these genes are affected.[8] The NF-κB pathway inhibitor *TNFAIP3* is commonly affected by (chromosomal) deletion and hypermethylation of the second allele,[7,9] while the *CD79B*, *CARD11*, and *MYD88* genes are frequently targeted by mutations that lead to activation of the NF-κB pathway.[8,10,11] Together, these results suggest that activation of the NF-κB pathway is involved in the pathogenesis of ABC-type DLBCL and that this pathway can serve as a potential therapeutic target in DLBCL. Indeed, several molecules in the NF-κB pathway have already been selectively targeted *in vitro* and *in vivo* to explore potential new treatment strategies, including SYK (fostamatinib),[12] BTK (ibrutinib),[13,14] PKCβ (enzastaurin/sotrastaurin),[15,16] and MALT1 (phenothiazines).[17,18] Moreover, the mutational status of espe-

cially *CARD11* and *CD79B* and to a lesser extent *MYD88* has been linked to sensitivity or resistance to drugs targeting the NF-κB pathway,[15,19] and their role therefore seems essential in tumor cell survival in nodal ABC-type DLBCL. We performed a comprehensive investigation of genetic aberrancies in PCLBCL-LT leading to pathological NF-κB pathway activation, to evaluate whether aberrant NF-κB activation is operative in this type of lymphoma.

Materials & Methods

Sample collection

Frozen biopsy primary tumor material of 10 PCLBCL-LT cases was available from the archive of the Leiden University Medical Center (Leiden, The Netherlands). A diagnosis of PCLBCL-LT was made according to criteria of the WHO-EORTC[20] and WHO classification,[21] and confirmed by a panel of hematopathologists and dermatologists, aided by several routinely performed immunohistochemical stainings. Cases were only included when frozen biopsy material contained a tumor cell percentage of at least 75%, as assessed by immunohistochemical stainings for CD20 and CD3. In all cases physical examination, total blood count, computed tomography scan, and bone marrow did not show extracutaneous disease at inclusion. Patient characteristics are summarized in Supplemental Table 1.

Activated B-cells

Human B-cells were purified from the separate lymphocyte fractions of peripheral blood (buffy coats) obtained from four healthy individuals by positive selection with magnetic CD19 MicroBeads (Miltenyi Biotec, Bergisch Gladbach, Germany). The B-cells were cultured in RPMI 1640 with 10% FCS and incubated with CpG (5 µg/ml) (ODN 2006, Invivogen, San Diego, USA) and monoclonal antibodies to CD40 (0.1 µg/ml) (BD Biosciences Pharmingen, Heidelberg, Germany) for 24 hours. After harvesting, a B-cell purity of more than 97% was confirmed by flow cytometric analysis with a mixture of monoclonal antibodies against B-cell (CD20, APC-H7), T-cell (CD3, PE-H7) and monocytes (CD14, APC). Simultaneously, the activation status was determined using anti-CD80 (PE) and anti-CD86 (FITC)), respectively. All antibodies were obtained from BD Biosciences. Dead cells were excluded using 1 µM of DAPI. A BD Biosciences LSRII was used for acquisition. WinList 7 (Verity Software House, Topsham, ME, USA) was used for data analysis. Approximately 86% of the lymphocytes showed expression of these activation markers.

DNA and RNA isolation

Genomic DNA was extracted using the Genomic-tip 20/G method, according to the protocol supplied by the provider (Qiagen, Hilden, Germany). RNA was isolated by the TRIzol method (Life Technologies, Carlsbad, CA, USA). 0,5 µg of total RNA was treated with RQ1 DNase I (Promega, Madison, WI) and reverse-transcribed by use of the iScript cDNA Synthesis kit (Bio-Rad, Veenendaal, The Netherlands).

TNFAIP3 gene expression

mRNA expression of *TNFAIP3* was analyzed by quantitative PCR (qPCR). Candidate reference genes were selected by analysis of gene expression data of two sets of (extra)nodal DLBCLs,[22,23]

online accessible in GENEVESTIGATOR (https:// www.genevestigator.com) and supplemented with three additional stably expressed reference genes, previously used by our group. Optimal reference genes were selected and tested as previously described.[24] The combination of *TMEM222*, *ZDHCC5*, and *ARF5*was identified as most optimal and used as reference gene set in all subsequent experiments. The qPCR reactions were run in triplicate with the use of iQ SYBR Green SuperMix (Bio-Rad) on the CFX384™ Real-Time System (Bio-Rad). The output data were analyzed using Bio-Rad CFX Manager software applying the ΔΔCq method. Relative expression was normalized to the determined reference gene set. Cycle parameters for all transcripts analyzed were as follows: denaturing for 15 seconds at 95 °C, and annealing and extension for 20 seconds at 60 °C, for 40 cycles. Specificity of the PCR products was confirmed by melting curve analysis. Primer sequences are listed in Supplemental Table 2.

TNFAIP3 copy number variation

A custom designed high-density fine-tiling DNA array with a resolution of 10 kB was set up for the genomic region of *TNFAIP3* (situated at chr6: 138,188,581-138,204,445; array coverage: chr6: 137,200,000- 139,200,000), according to the human genome, built 19 (February 2009; Humane Genome Browser, University of California, Santa Cruz, CA, USA). The array was prepared using Maskless Array Synthesizer Technology (NimbleGen Systems, Reykjavik, Iceland). The mean fluorescence was normalized to reference DNA (healthy donor DNA from blood, Promega, Madison, USA) and analyzed using SignalMap software (NimbleGen Systems) in order to detect copy number alteration in the chromosomal region containing the *TNFAIP3* locus.

TNFAIP3 promoter methylation assay

Using the EZ Methylation Kit (Zymo Research Corporation, Orange, CA), extracted tumor sample DNA was treated with sodium bisulfite. PCR primers annealing to sodium bisulfite-modified DNA, 5'- ATTGAAACGGGGTAAAGTAGATTG - 3' forward and 5'- CAAAATCCCAAATCCTAATCAAAACA - 3' reverse, were designed. Primers were developed in such a way that both methylated and unmethylated sequences are amplified using the same bisulfite treated DNA as PCR template. These primers amplified a 236 bp genomic region (-211 bp to +26 bp from the transcription start site (ENST00000237289)) and covering the middle part of the promoter CpG island of *TNFAIP3*. Twenty-four CpGs were situated in this amplicon. PCR amplification was performed on the CFX384™ Real-Time System (Bio-Rad), and afterwards melting curves were acquired in the presence of iQ SYBR Green Supermix (Bio-Rad) during a linear temperature transition from 65 to 90 °C with increments of 0,2 °C per 10 seconds. The presence of methylated DNA in the samples was detected through a peak with a higher melting curve temperature (84.2 °C) as compared to unmethylated DNA (79.6 °C), using bisulfite converted unmethylated human semen DNA and methylated human DNA (Chemicon, Hampshire, UK) as references as described before.[24]

TNFAIP3 alternative transcript analysis

For isolated tumor sample DNA, the genomic region containing exons 3 and 4 and intron 3 of *TNFAIP3* was amplified. Forward primer 5'- TTGCTGGGTCTTACATGCAG- 3' and reverse primer 5'- GCTGAAAGCATTTAAGTACAGATCC- 3' were designed for PCR amplification in the presence of Advantage GC Genomic LA Polymerase Mix (Clontech, Heidelberg, Germany). PCR products

were sequenced by the 3730XL/3130XL Genetic Analyzer (LGC Genomics, Berlin, Germany). The nucleotide alterations of each gene were analyzed using Mutation Surveyor software (Softgenetic, State College, PA).

For cDNA amplification of *TNFAIP3* exon 3 to 5, 5'- ATTTGTTGAAACGGGGCTTT- 3' forward and 5'- GGCGAAATTGGAACCTGAT- 3' reverse primers were designed. Amplification was performed on the C1000 Touch™ Thermal Cycler (Bio-Rad) using a touchdown PCR protocol with the following parameters: denaturing at 95°C for 30 seconds, followed by 40 cycles of annealing at 65 °C to 58 °C for 20 seconds (with a 1 °C decrement per cycle in the first 7 cycles) and extension at 72 °C for 30 seconds. The purified PCR products were subjected to Sanger sequencing both with forward and reverse primers on the ABI 3730 (Applied Biosystems, Foster City, CA). The sequenced PCR fragments of each gene were aligned to the corresponding normal sequences (Ensembl Genome Browser 70, http://www.ensembl.org).

Mutational analysis of CD79B and CARD11, and MYD88

PCR was performed to amplify exon 5 of *CD79B*, exons 5 to 10 of *CARD11*, and exon 5 of *MYD88* for both DNA and cDNA (primer pairs listed in Supplemental Tables 2 and 3), on the C1000 Touch™ Thermal Cycler (Bio-Rad) using the touchdown PCR protocol as described above. The PCR products were completely sequenced in both directions on the ABI 3730 (Applied Biosystems). Mutation Surveyor software (SoftGenetic) was used for analysis of single nucleotide alterations.

Results

TNFAIP3

mRNA expression of *TNFAIP3* varied substantially among the tumor samples (Figure 1) as measured relative to stably expressed reference genes *TMEM222*, *ZDHCC5*, and *ARF5*. The high-density fine-tiling DNA array showed decreased mean fluorescence in the *TNFAIP3* chromosomal region in four tumor samples. The mean log2 transformed fluorescence levels of these samples varied from-0,315 to-0,382 and were concordant with heterozygous deletion of the gene region. Above that, in all 4 samples the complete region investigated (1 MB upstream and downstream of the gene) was heterozygously deleted, confirming this deletion targeted a larger chromosomal area than the *TNFAIP3* locus alone.

Mutational analysis CD79B, CARD11, and MYD88

Two tumor samples showed a nucleotide substitution in the first immunoreceptor tyrosine-based activation motif (ITAM) of *CD79B*, the first one a c.680A>T missense mutation leading to substitution of tyrosine by phenylalanine (Y196F), the second one a c.679T>C mutation in which tyrosine will be substituted by histidine (Y196H). Both mutations were detected at genomic and transcriptional level (Supplemental Figure 1a and b).

One tumor sample showed both a c.1649C>A and a c.1671C>T mutation in *CARD11* in DNA and cDNA (Supplemental Figure 1c), leading to a substitution of aspartic acid by glutamic acid (D415E), and of arginine by tryptophan (R423W), respectively. Two additional tumor samples showed alterations in codon 415 of CARD11, concerning a similar silent mutation (c.1649C>T)

(Supplemental Figure 1d). One of these samples displayed this mutation in DNA and cDNA sequences. For the other sample, only cDNA was analyzed.

Figure 1. *TNFAIP3* mRNA expression (quantitative PCR)

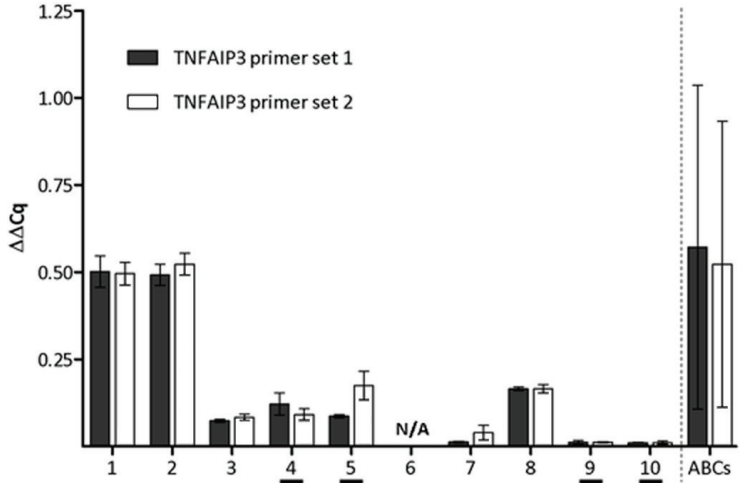

Mean ΔΔCq for PCR with two primer sets for TNFAIP3 relative to reference genes TMEM222, ZDHHC5 and ARF5 for 9 of 10 tumor samples and 4 samples of in vitro activated peripheral blood B-cells (ABCs). The error bars represent the standard deviation. The underlined tumor samples showed heterozygous deletion of the complete TNFAIP3 gene region.

Methylation-specific melting curve analysis of the *TNFAIP3* promoter region showed melt curves at the temperature of unmethylated control DNA in all 9 tumor samples tested. No *TNFAIP3* intron 3 mutations or gene conversions affecting the intronic c.487-2A to c.487-1G acceptor splicing site were detected. In cDNA, PCR amplification of exon 3 to 5 of TNFAIP3 using cDNA showed normal transcripts with a length of 212 base pairs and without replacement any of these exons.

In of four cases, a c.794T>C mutation in *MYD88* was detected in DNA (Supplemental figure 1e and f), leading to a substitution of leucine by proline (L265P). This specific mutation was also present in cDNA in 3 of these cases, but one of these four showed an unchanged cDNA sequence.

An overview of all results is given in Table 1, showing that 7 out of 10 cases contained genetic alterations involved in the regulation of the NF-κB pathway that could lead to constitutive activation of this signaling pathway. Off note, one of the three cases without genetic alterations showed relatively low levels of *TNFAIP3*, suggesting that NF-κB pathway activation is also present in these tumors. In this relatively small cohort of PCLBCL-LT cases, no correlation between genetic aberrancies and survival was found.

Discussion

We generated a comprehensive overview of NF-κB-activating genetic aberrancies in PCLBCL-LT. Evident genetic alteration were encountered in 7 out of 10 samples, strongly suggesting that constitutive activation of the NF-κB pathway plays a role in the pathogenesis and/or tumor cell survival in PCLBCL-LT.

TNFAIP3

TNFAIP3 (A20) is a tumor suppressor gene, downregulating the NF-κB signaling pathway by deubiquitination of several target proteins involved in activation of this pathway. The TNFAIP3 protein consists of an ovarian tumor (OTU) domain and seven Zinc finger domains, both necessary for optimal functioning.[25] In both nodal ABC-type DLBCL and PCLBCL-LT, chromosomal arm 6q, on which the *TNFAIP3* gene is situated, is frequently deleted.[26,27]

Table 1. Overview of genetic aberrancies

	TNFAIP3 / A20					**CD79B**		**CARD11**		**MYD88**	
	del.	hyper-methy-lation	qPCR (ΔΔCq)	splicing site		Y196 ITAM mutation		coiled-coil domain mutation		L265P mutation	
				mut.	*splice variant*	*DNA*	*cDNA*	*exon 5-8 & 10*	*exon 9*	*DNA*	*cDNA*
1	no	no	0,50	no	no	no	no	no	no	L265P	L265P
2	no	no	0,51	no	no	no	no	no	no	no	no
3	no	no	0,08	no	no	no	no	no	no	no	no
4	+/-	no	0,11	no	no	no	no	no	no	L265P	L265P
5	+/-	no	0,13	no	no	no	no	no	D415E, R423W	no	no
6	no	no	N/A	N/A	N/A	no	no	no	no[1]	no	no
7	no	N/A	0,03	no	no	Y196H	Y196H	no	no	L265P	no
8	no	no	0,17	no	no	Y196F	Y196F	no	no	L265P	L265P
9	+/-	N/A	0,01	no	no	N/A	no	no	no	N/A	no
10	+/-	no	0,01	no	no	no	no	no	D415D	no	no

del: deletion; mut: mutation; +/-: heterozygous deletion; N/A: not assessed; [1] A silent mutation (D415D) was detected.

As the mRNA expression levels of *TNFAIP3* varied amongst the tumor samples of PCLBCL-LT, we were interested in potential underlying mechanisms for these variations in PCLBCL-LT. Four cases showing heterozygous deletion of the gene region indeed showed relatively low mRNA expression levels of *TNFAIP3*. These heterozygous deletions were concordant with our previous results of conventional array comparative genomic hybridization studies in primary cutaneous large B-cell lymphomas.[26] Homozygous deletions that are observed in 10% of nodal ABC-type DLBCL,[7] were not found in PCLBCL-LT. In cases with two gene copies of *TNFAIP3* and relatively low levels of mRNA, we could not establish a negative regulatory mechanism. Epigenetic silencing through promoter hypermethylation was not detected in PCLBCL-LT, as was encountered in approximately 40 percent of nodal ABC-type DLBCLs.[9] Furthermore, we investigated whether the *TNFAIP3* transcripts present could give rise to functional proteins. In one-third of cases of nodal ABC-type DLBCL, intron 3 splice site mutations or gene conver-

sions disrupting the intron 3 splice site are encountered, leading to transcripts with an introduced premature stop codon. These transcripts will give rise to a truncated protein without the essential OUT and Zinc finger domains. Again we could not detect these alterations in PCLBCL-LT. As TNFAIP3 was demonstrated to influence proliferation and survival in normal B-cells in a gene-dose-dependent fashion,[28] the relatively low expression of *TNFAIP3* in most of the PCLBCL-LT samples still seems a relevant finding.

Altogether, the heterozygous deletions of *TNFAIP3* and reduced mRNA expression in PCLBCL-LT suggest a role for this tumor suppressor in the pathogenesis of this type of lymphoma, but the mechanisms of reduced expression of *TNFAIP3* are different from the ones encountered in nodal ABC-type DLBCL.

CD79B, CARD11 and MYD88 activating mutations

CD79B (immunoglobulin-associated beta) is a component of the B-cell receptor, and has a combined function with CD79A in the assembly and membrane expression of the B-cell receptor. The CD79A/CD79B heterodimer also initiates downstream activation of different signaling pathways, including the NF-kB pathway.[29] Somatic mutations affecting *CD79B* were detected in 18% of nodal ABC-type DLBCLs, mainly comprising recurrent mutations in the first immunoreceptor tyrosine-based activation motif (ITAM) tyrosine Y196. These mutations lead to increased surface B-cell receptor expression and downregulated Lyn kinase, a feedback inhibitor of B-cell receptor signaling.[10] The mechanism of activation of the NF-κB pathway through these mutations is called chronic active B-cell receptor signaling, and occurs in cases with wild-type *CARD11*. In our series, concordant with nodal ABC-type DLBCLs, in 20% an Y196 mutation was detected in the absence of mutations in *CARD11*, suggesting that chronic active B-cell receptor signaling is a mechanism involved in these cases of PCLBCL-LT.

CARD11 is a signaling scaffold protein involved in coordinating the activation of the NF-kB pathway,[11] and a critical component involved in constitutive NF-κB activation in ABC-DLBCL,[6] downstream of the B-cell receptor (see Figure 2).Remarkably, in 3 out of 10 cases, we found point mutations in codon 415 of exon 9. In two of these cases, it concerned a silent mutation. Although functional consequences may seem less apparent for silent mutations, there is increasing evidence that these do have physiological effects, for example through incorrect splicing and changes in RNA structure or by altering the rate of translation.[30] However, as this mutation is a common single nucleotide polymorphism, the relevance of these mutations in PCLBCL-LT can be debated. The sample with a missense mutation in this codon (D415E) also showed a R423W mutation in the same exon in both DNA and cDNA. This *CARD11* R423W mutation was previously described in nodal ABC-type DLBCL.[7] In contrast to some known *CARD11* mutations, the functional relevance of the D415E and R423W mutations has not yet been investigated. However, mutations in the coiled-coil domain are potentially relevant in constitutive activation of the NF-κB pathway, as changes in this domain have the potential to disrupt the autoinhibition of CARD11 signaling, leading to receptor-independent activation of the NF-κB pathway.[31]

Myeloid response gene 88 (MYD88) is a Toll-like receptor associated adaptor protein with many cellular functions. Amongst others, MYD88 is known to be involved in activation of different signaling pathways through the assembly of a complex containing IRAK1 and IRAK4.[8] Nodal ABC-type DLBCLs showed a L265P mutation in 29% of cases, and the consequent amino acid substitution in the βD sheet of MYD88 has been shown to be oncogenically active,

leading to aberrant activation of NF-κB and JAK-STAT3 signaling pathways and lymphoma cell survival,[8] a mechanism most likely not directly related to (chronic active) B-cell receptor signaling (see Figure 2). In primary central nervous system DLBCL, also an extranodal DLBCL of ABC-genotype, the L265P mutation was encountered in 36% of cases[32] and 38% of cases[33]. Somatic *MYD88* L265P mutations in PCLBCL-LT have been previously described in 69% of cases.[34] The 40% mutation rate we encountered in our series is therefore concordant with other (extra)nodal ABC-type DLBCLs. Furthermore, we showed that not all mutations in the DNA seem to be transcribed to RNA, as for one sample, the mutation was not detected in cDNA.

Table 2. Genetic aberrancies in PCLBCL-LT compared to nodal ABC-type DLBCL

	PCLBCL-LT	**nodal ABC-type DLBCL**
CD79B ITAM mutations	20%	20%
CARD11 coiled-coil domain mutations	10%	10%
MYD88 L265P mutation	30%*	40%
TNFAIP3		
- homozygous deletion	0%	10%
- heterozygous deletion	40%	40%
- epigenetic silencing	0%	40%
- alternative transcripts	0%	33%

*30% in cDNA, 40% in DNA

PCLBCL-LT, primary cutaneous large B-cell lymphoma, leg type; ABC-type DLBCL, activated B-cell-type diffuse large B-cell lymphoma

Mutational status and therapeutic targets

The above described specific mutations not only give more insight into the pathogenesis of (extra)nodal DLBCLs, but the relevance of these mutations for novel therapeutic strategies has also been explored. For example, sotrastaurin can interfere with NF-κB pathway activation, by inhibition of PKC-β, which is required for CARD11-dependent activation of the NF-κB pathway.[35] Sotrastaurin was shown to be selectively toxic for *CD79*-mutant DLBCL in a mouse xenograft model[15] as compared to unmutated DLBCL, but only in presence of wild-type *CARD11*. These findings strongly suggest that sotrastaurin is especially promising in cases of DLBCL with chronic active B-cell receptor signaling. An RNA interference screen revealed that a BCR signaling component, Bruton's tyrosine kinase (BTK), is essential for the survival of nodal ABC-type DLBCL with wild-type CARD11 and in addition, knockdown of proximal B-cell receptor units, i.e. CD79B, was selectively toxic to wild-type *CARD11* nodal ABC-type DLBCL, but not to other lymphomas.[10] Furthermore, in a phase I trial, the BTK-inhibitor ibrutinib was well-tolerated and generated a clinical (partial) response in 40% of refractory nodal ABC-type DLBCL, both in patients with tumors bearing *CD79* mutations or a combination of *CD79* and *MYD88* mutations. However, patients with only *MYD88* mutations were refractory to this treatment, reflecting the B-cell receptor signaling-independency of these MYD88-mutated tumors and warranting assessment of the mutations status of these NF-κB related signaling molecules.[19]

In conclusion, seven out of ten cases of PCLBCL-LT showed genetic alterations in the NF-κB pathway. For pathway-activating mutations in the *CD79B* ITAM, *MYD88* L265P mutations and *CARD11* coiled-coil domain mutations, the percentage of tumors affected corresponds to the percentages in nodal ABC-type DLBCL (Table 2). However, although downregulated mRNA expression of *TNFAIP3* in our samples was highly suggestive for a role of this tumor suppressor in NF-κB activation, the genetic substrate for low expression is not completely evident in PCLBCL-LT, and therefore differs from the well-defined mechanisms downregulating the function of TNFAIP3 in nodal ABC-type DLBCL. Together, these findings strongly suggest a role for constitutive activation of the NF-κB pathway in PCLBCL-LT, and provide the rationale to explore the possibility of using specific therapy targeted at components of the NF-κB pathway in this type of lymphoma.

Figure 2. Pathway overview and genetic aberrancies in primary cutaneous large B-cell lymphoma, leg type

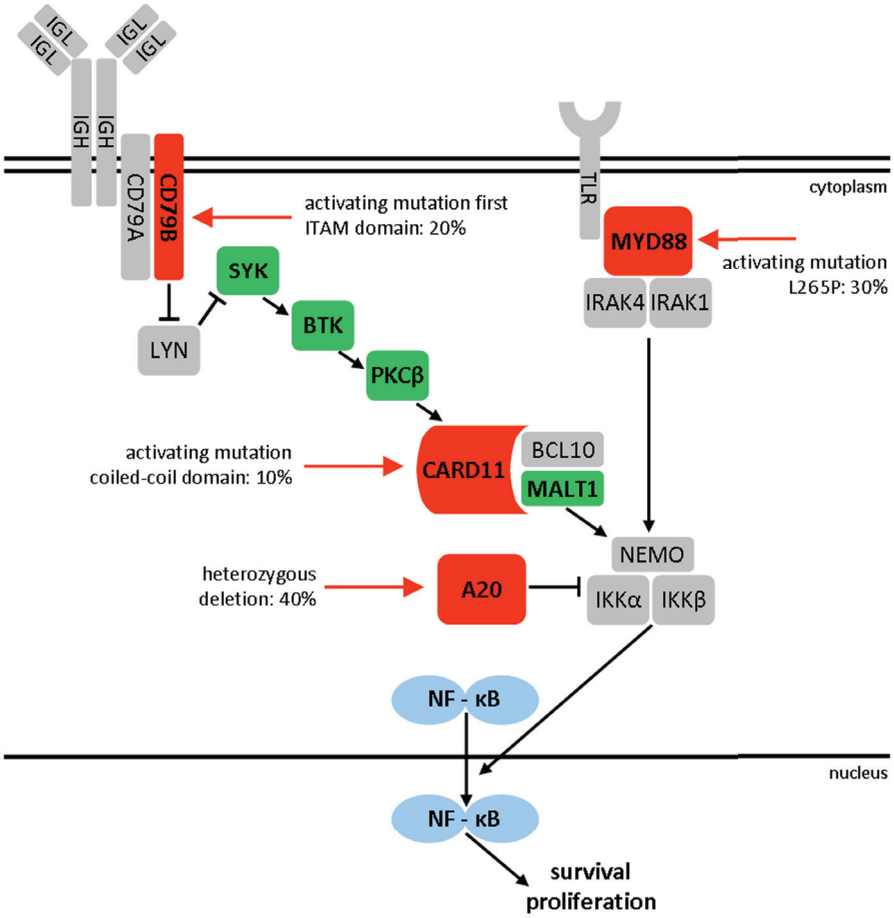

The suggested relations between the different components of B-cell receptor signaling and MYD88 signaling are represented.[14] The molecules affected by genetic aberrancies in PCLBCL-LT are indicated in red and the percentage of the cases affected by these aberrancies are indicated. Molecules that can be therapeutically targeted for inhibition of the NF-κB pathway are represented in green.

References

1. Vermeer MH, Geelen FA, van Haselen CW, et al. (1996) Primary cutaneous large B-cell lymphomas of the legs. A distinct type of cutaneous B-cell lymphoma with an intermediate prognosis. Dutch Cutaneous Lymphoma Working Group. Arch Dermatol 132: 1304-8.

2. Senff NJ, Noordijk EM, Kim YH, et al. (2008) European Organization for Research and Treatment of Cancer and International Society for Cutaneous Lymphoma consensus recommendations for the management of cutaneous B-cell lymphomas. Blood 112: 1600-9.

3. Davis RE, Brown KD, Siebenlist U, et al. (2001) Constitutive nuclear factor kappaB activity is required for survival of activated B cell-like diffuse large B cell lymphoma cells. J Exp Med 194: 1861-74.

4. Grumont RJ, Gerondakis S. (2000) Rel induces interferon regulatory factor 4 (IRF-4) expression in lymphocytes: modulation of interferon-regulated gene expression by rel/nuclear factor kappaB. J Exp Med. 191: 1281-92.

5. Hoefnagel JJ, Dijkman R, Basso K, et al. (2005) Distinct types of primary cutaneous large B-cell lymphoma identified by gene expression profiling. Blood 105: 3671-8.

6. Ngo VN, Davis RE, Lamy L, et al. (2006) A loss-of-function RNA interference screen for molecular targets in cancer. Nature 441: 106-10.

7. Compagno M, Lim WK, Grunn A, et al. (2009) Mutations of multiple genes cause deregulation of NF-kappaB in diffuse large B-cell lymphoma. Nature 459: 717-21.

8. Ngo VN, Young RM, Schmitz R, et al. (2011) Oncogenically active MYD88 mutations in human lymphoma. Nature 470: 115-9.

9. Honma K, Tsuzuki S, Nakagawa M, et al. (2009)TNFAIP3/A20 functions as a novel tumor suppressor gene in several subtypes of non-Hodgkin lymphomas. Blood 114: 2467-75.

10. Davis RE, Ngo VN, Lenz G, et al. (2010) Chronic active B-cell-receptor signalling in diffuse large B-cell lymphoma. Nature 463: 88-92.

11. Lenz G, Davis RE, Ngo VN, et al. (2008) Oncogenic CARD11 mutations in human diffuse large B cell lymphoma. Science 319: 1676-9.

12. Friedberg JW, Sharman J, Sweetenham J, et al. (2010) Inhibition of Syk with fostamatinib disodium has significant clinical activity in non-Hodgkin lymphoma and chronic lymphocytic leukemia. Blood 115: 2578-85.

13. Advani RH, Buggy JJ, Sharman JP, et al. (2013) Bruton tyrosine kinase inhibitor ibrutinib (PCI-32765) has significant activity in patients with relapsed/refractory B-cell malignancies. J Clin Oncol 31: 88-94.

14. Yang Y, Shaffer AL, III, Emre NC, et al. (2012) Exploiting synthetic lethality for the therapy of ABC diffuse large B cell lymphoma. Cancer cell 21: 723-37.

15. Naylor TL, Tang H, Ratsch BA, et al. (2011) Protein kinase C inhibitor sotrastaurin selectively inhibits the growth of CD79 mutant diffuse large B-cell lymphomas. Cancer Res 71: 2643-53.

16. Robertson MJ, Kahl BS, Vose JM, et al. (2007) Phase II study of enzastaurin, a protein kinase C beta inhibitor, in patients with relapsed or refractory diffuse large B-cell lymphoma. J Clin Oncol 25: 1741-6.

17. Fontan L, Yang C, Kabaleeswaran V, et al. (2012) MALT1 small molecule inhibitors specifically suppress ABC-DLBCL in vitro and in vivo. Cancer cell 22: 812-24.

18. Nagel D, Spranger S, Vincendeau M, et al. (2012) Pharmacologic inhibition of MALT1 protease by phenothiazines as a therapeutic approach for the treatment of aggressive ABC-DLBCL. Cancer cell 22: 825-37.

19. Wilson WH, Gerecitano JF, Goy A, et al. (2012) The Bruton's Tyrosine Kinase (BTK) Inhibitor, Ibrutinib (PCI-32765), Has Preferential Activity in the ABC Subtype of Relapsed/Refractory De Novo Diffuse Large B-Cell Lymphoma (DLBCL): Interim Results of a Multicenter, Open-Label, Phase 2 Study. Blood (ASH Annual Meeting Abstracts) 120: 4039.

20. Willemze R, Jaffe ES, Burg G, et al. (2005) WHO-EORTC classification for cutaneous lymphomas. Blood 105: 3768-85.

21. Meijer CJLM, Vergier B, Duncan LM, et al. (2008) Primary cutaneous DLBCL, leg type. In: Swerdlow SH, Campo E, Harris NL, et al., eds. WHO classification of tumours of haematopoietic and lymphoid tissues. Lyon: IARC Press 242.

22. Booman M, Szuhai K, Rosenwald A, et al. (2008) Genomic alterations and gene expression in primary diffuse large B-cell lymphomas of immune-privileged sites: the importance of apoptosis and immunomodulatory pathways. J Pathol 216: 209-17.

23. Lenz G, Wright GW, Emre NC, et al. (2008) Molecular subtypes of diffuse large B-cell lymphoma arise by distinct genetic pathways. Proc Natl Acad Sci USA 105: 13520-5.

24. van Kester MS, Borg MK, Zoutman WH, et al. (2012) A meta-analysis of gene expression data identifies a molecular signature characteristic for tumor-stage mycosis fungoides. J Invest Dermatol 132: 2050-9.

25. Wertz IE, O'Rourke KM, Zhou H, et al. (2004) De-ubiquitination and ubiquitin ligase domains of A20 downregulate NF-kappaB signalling. Nature 430: 694-9.

26. Dijkman R, Tensen CP, Jordanova ES, et al. (2006) Array-based comparative genomic hybridization analysis reveals recurrent chromosomal alterations and prognostic parameters in primary cutaneous large B-cell lymphoma. J Clin Oncol 24: 296-305.

27. Tagawa H, Suguro M, Tsuzuki S, et al. (2005) Comparison of genome profiles for identification of distinct subgroups of diffuse large B-cell lymphoma. Blood 106: 1770-7.

28. Chu Y, Vahl JC, Kumar D, et al. (2011) B cells lacking the tumor suppressor TNFAIP3/A20 display impaired differentiation and hyperactivation and cause inflammation and autoimmunity in aged mice. Blood 117: 2227-36.

29. Dal Porto JM, Gauld SB, Merrell KT, et al. (2004) B cell antigen receptor signaling 101. Mol Immunol 41: 599-613.

30. Sauna ZE, Kimchi-Sarfaty C. (2011) Understanding the contribution of synonymous mutations to human disease. Nature reviews Genetics 12: 683-91.

31. Lamason RL, McCully RR, Lew SM, et al. (2010) Oncogenic CARD11 mutations induce hyperactive signaling by disrupting autoinhibition by the PKC-responsive inhibitory domain. Biochemistry 49: 8240-50.

32. Montesinos-Rongen M, Godlewska E, Brunn A, et al. (2011) Activating L265P mutations of the MYD88 gene are common in primary central nervous system lymphoma. Acta Neuropathol 122: 791-2.

33. Gonzalez-Aguilar A, Idbaih A, Boisselier B, et al. (2012) Recurrent mutations of MYD88 and TBL1XR1 in primary central nervous system lymphomas. Clin Cancer Res 18: 5203-11.

34. Pham-Ledard A, Cappellen D, Martinez F, et al. (2012) MYD88 somatic mutation is a genetic feature of primary cutaneous diffuse large B-cell lymphoma, leg type. J Invest Dermatol 132: 2118-20.

35. Sommer K, Guo B, Pomerantz JL, et al. (2005) Phosphorylation of the CARMA1 linker controls NF-kappaB activation. Immunity 23: 561-74.

Supplemental Table 1. Patient characteristics

	Sex	Age at diagnosis (years)	Skin site of primary tumor	Immunohistochemistry					Initial therapy	Disease recurrence	PFS (months)	Follow-up (months)	Current status
				BCL2	BCL6	CD10	IRF4/ MUM1	B-cell receptor					
1	m	84	legs + other	+	+	-	+	IgM IgD κ	RT	yes	1	24	D^+
2	f	75	both legs	+	+	-	+	IgM λ	PCT + RT	yes	12	54	D^+
3	f	79	leg	+	+	-	+	IgM κ	RT	no	20	21	A^0
4	f	81	leg	+	-	-	+	IgM IgD	PCT + RT	yes	20	39	D^+
5	m	81	leg	+	+	-	+	IgM IgD λ	none	no	0	2	D^+
6	m	53	legs + other	+	+	-	+	IgM κ	PCT	yes	6	96	A^+
7	m	68	leg	+	+	-	+	IgM IgD λ	PCT	yes	17	60	D^+
8	f	83	leg	+	+	-	+	IgM IgD κ	PCT + RT	yes	34	38	D^+
9	m	83	leg	+	+	-	+	IgM IgD κ	RT	no	49	50	A^0
10	f	76	leg	+	-	+	+	IgM κ	RT	no	0	13	D^+

m: male; f: female; PFS: progression-free survival; RT: radiotherapy; PCT: polychemotherapy; A^+: alive with disease; A^0: alive without disease; D^+: death with disease.

Supplemental Figure 1. Sequencing results of *CD79B*, *MYD88*, and *CARD11*

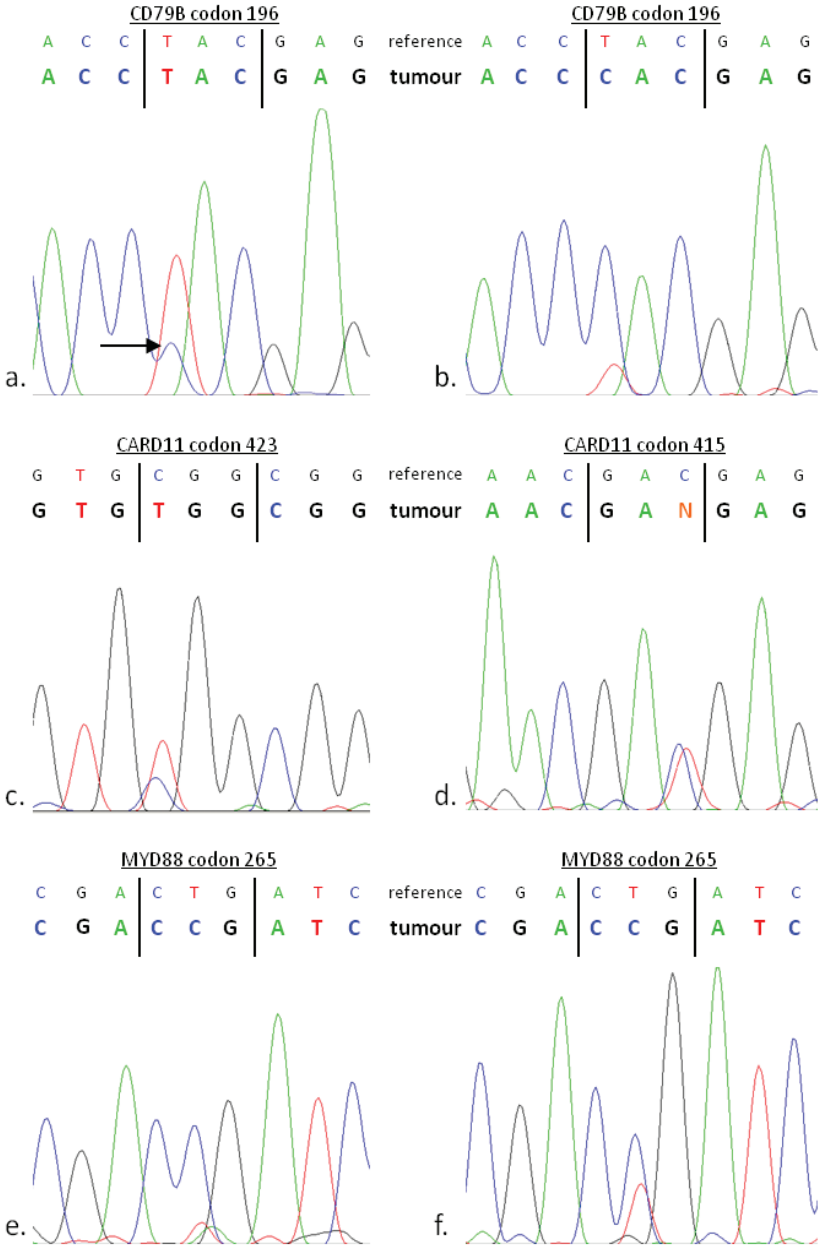

DNA (a) and cDNA (b) sequences of *CD79B* exon 5 in tumor sample 8, concordant with a Y196H mutation. Although in DNA, the dominant sequence of codon 196 is equal to the reference sequence, a clear C-peak is visible under the T-peak (arrow), indicating a nucleotide substitution. In cDNA of the same tumor, the C-peak is dominant, suggesting a predominant expression of the mutated allele. cDNA sequence of *CARD11* exon 9 of tumor sample 5 showing a R423W mutation (c) and of tumor sample 6 with a silent mutation in codon 415 (d). DNA (e) and cDNA (f) sequences of *MYD88* exon 5 in tumor sample 4 showing a L265P mutation.

Supplemental Table 2. Primers for quantitative PCR

Gene		Sequence 5'- 3'	Product size
TNFAIP3 (1)[1]	- forward	CTGGGACCATGGCACAACTC	182 bp
	- reverse	CGGAAGGTTCCATGGGATTC	
TNFAIP3 (2)	- forward	CCATGGCACAACTCATCTCA	172 bp
	- reverse	GAAGGTTCCATGGGATTCTG	
TMEM222	- forward	CGCCTCTGAGGAGTACAAGC	92 bp
	- reverse	TGTAGCGCATCAGATTCAGG	
ARF5	- forward	TGCTGATGAACTCCAGAAGATGC	144 bp
	- reverse	CGGCTGCGTAAGTGCTGTAG	
ZDHCC5	- forward	TATCGGCCGGGTTACAGTAG	95 bp
	- reverse	GTTGGCTCCTTCAAGCTGTC	

1. Braun FCM, Grabarczyk P, Möbs M, et al. (2011) Tumor suppressor TNFAIP3 (A20) is frequently deleted in Sézary syndrome. Leukemia 25: 1494-1501.

Supplemental Table 3. Primers for mutational analysis DNA

Gene			Sequence 5'- 3'	Product size
CD79B	- forward		TCTTGCAGAATGCACCTCAC	159 bp
	- reverse		CCAACCACACCAGCAGATAG	
MYD88 [2]	- forward		CTGGGGTTGAAGACTGGGCT	276 bp
	- reverse		TGGACAGGCAGACAGATAC	
CARD11 [3]	exon 5	- forward	CAGTGCCTCGTGGGCAGAGT	502 bp
		- reverse	GTCACCCTGGCGGAGTAGCC	
	exon 6	- forward	CTGGAGAAGGTTTCTTGGAGC	425 bp
		- reverse	ACACCCTGGCAGGTTCATC	
	exon 7	- forward	CCCAGGATACGCCCAAGCAA	593 bp
		- reverse	CCCAGGCCCTCATCTGGTTG	
	exon 8	- forward	TCCCCTATGTTACCTGGTCTGTAGTG	573 bp
		- reverse	GCCTGTGACTTCCAAAAAAGCC	
	exon 9	- forward	CCTCAGTGCCCTCATCTGTAAAATG	765 bp
		- reverse	CAAAGGACAAGGAGCCATTCATTG	
	exon 10	- forward	CCAGAAGCCTGGGAGGAGGA	564 bp
		- reverse	AGCGAGTCGCAGGATTTCCA	

2. Pham-Ledard A, Cappellen D, Martinez F, et al. (2012) MYD88 somatic mutation is a genetic feature of primary cutaneous diffuse large B-cell lymphoma, leg type. J Invest Dermatol 132: 2118-20
3. Lenz G, Davis RE, Ngo VN, et al. (2008) Oncogenic CARD11 mutations in human diffuse large B-cell lymphoma. Science 319: 1676-9.

Supplemental Table 4. Primers for mutational analysis cDNA

Gene			Sequence 5'- 3'	Product size
CD79B	- forward		AGTCATGGGATTCAGCACCT	218 bp
	- reverse		GCAGCGTCACTATGTCCTCA	
MYD88	- forward		AGGAGATGATCCGGCAACT	297 bp
	- reverse		CGCAGACAGTGATGAACCTC	
CARD11	exon 9	- forward	AATGTACAAGCACCGCATGA	295 bp
		- reverse	GATGGTTACTGGCAGGTTCC	